

IMECE2005-79766

TIME-RESOLVED MICROSCALE TEMPERATURE MEASUREMENTS OF HIGH-POWER SEMICONDUCTOR LASERS

Paddy K.L. Chan¹, Amul D. Sathe¹, Kevin P. Pipe¹,
Jason J. Plant² and Paul W. Juodawlkis²

¹Department of Mechanical Engineering, University of Michigan, Ann Arbor, MI, USA

²Lincoln Laboratory, Massachusetts Institute of Technology, Lexington, MA, USA

ABSTRACT

Nonradiative recombination and other heat generation processes affect both the performance and lifetime characteristics of semiconductor diode lasers. This is especially true for high-power devices, where facet heating due to nonradiative recombination can lead to catastrophic optical damage (COD). Here we present for the first time temperature measurements of a semiconductor laser in which the surface temperature profile (and hence the current density profile) of the laser is measured as it evolves in time. The laser studied is a $\lambda=1.55\mu\text{m}$ 1-cm-long InGaAsP/InP watt-class slab-coupled optical waveguide laser (SCOWL). The ridge width of the SCOWLS examined here is approximately $5\mu\text{m}$. Temperature measurements are taken using multiple microthermocouples with sizes less than $20\mu\text{m}$. Surface temperature fluctuations in time are seen to be quite large, as high as 20% of the total temperature increase of the device. Time-resolved measurements allow us to see both positive correlation (in which the temperature rises at the same time across an area of the device) as well as negative correlation (in which part of the device gets hot at the same time as another part of the device gets cold). Negative correlations are likely due to facet heating processes which cause bandgap shrinkage and hence increased current flow to a facet, pulling current away from the center of the device. Time-resolved measurements of the surface temperature profile therefore show promise as a non-destructive method for characterizing the failure mechanisms of a laser, as facet damage over time is otherwise very difficult to measure before the COD runaway process destroys the device.

NOMENCLATURE

A	Laser top contact surface area (cm^2)
J	Current density (A/cm^2)
J_o	Average current density (A/cm^2)
k	Thermal conductivity ($\text{W}/\text{cm}\cdot\text{K}$)
P_{out}	Optical power output (W)
T	Temperature (K)
T_o	Average temperature (K)
T_{top}	Laser top contact surface temperature (K)
T_{sink}	Heat sink temperature (K)
V	Supply voltage (V)
γ	Size factor of thermocouple

INTRODUCTION

Catastrophic optical damage (COD) has been a long-standing problem in laser diodes¹⁻³. For high power lasers in particular, COD is one of the main factors that limit device lifetime⁴. Generally, COD is linked to a rapid increase in temperature at a laser facet due to nonradiative recombination and absorption of photons. The increase in facet temperature causes shrinkage of the energy bandgap, which then leads to current concentration at the facet and increased optical absorption and nonradiative recombination, thereby causing further increase of facet temperature. This positive feedback mechanism leads to thermal runaway until the facet temperature exceeds the melting point of the material and the laser output facet is destroyed. Thermal runaway is much less prevalent in aluminum-free lasers (such as the InGaAsP/InP structure examined here) because of reduced facet oxidation. While gradual degradation occurred over a long time period

(no sudden catastrophic damage was observed in the lasers used in this study), measuring the fluctuation of the injection current along the laser ridge can be a method to clarify the level of degrades before COD happens.

Here we directly examine the mechanism that leads to COD by profiling for the first time the spatial variation of current density injection across the laser top contact surface as it varies in time. In order to do this, we perform microscale temperature measurements on the laser surface with multiple microthermocouples, measuring temperature at a relatively short (0.33s) time scale and recognizing that temperature variations are intimately linked to current density fluctuations. In these measurements we look for both positive correlation (in which the temperature rises at the same time across an area of the device) as well as negative correlation (in which part of the device gets hot at the same time as another part of the device gets cold). Measurements indicate that top surface temperature fluctuations can be a large fraction of the time-averaged temperature difference between the laser surface and the heat sink. From the measured fluctuation in surface temperature near a facet, the variation of injected current density to the facet can be inferred.

EXPERIMENT

Photoluminescence and Raman scattering techniques are often utilized for facet temperature measurement⁴⁻⁷; however, using these techniques to measure temperature at several locations on a laser at once is difficult. CCD-based thermoreflectance can generate a microscale surface temperature profile, but its time resolution is limited due to the requirement of averaging a large amount of data⁸. In order to measure temperature at several locations at once with a time resolution less than 1 second, we use a microthermocouple-based probing technique which has previously been demonstrated for laser surface temperature measurements⁹. The thermocouple meter used to correlate the measured thermal voltage with temperature has a 3Hz sampling frequency, and the temperatures are recorded simultaneously using a computer equipped with LabVIEW. Three microthermocouples, each with an accuracy of 200mK and a resolution of 10mK, are placed at the 2 facets and center of the laser as shown in Fig.1. The laser is mounted on a copper block heat sink, the temperature of which is maintained in a feedback loop by a Peltier cooler, integrated thermistor, and temperature controller. The sample is a watt-class InGaAsP/InP slab-coupled optical waveguide laser (SCOWL) which has a tensile-strained multi-quantum well (MQW) active region with a thickness of 40nm¹⁰. The length of the device is 1 cm, and eighteen equally-spaced gold bond wires are located on the top surface to help facilitate evenly distributed current injection. The laser is biased by a current source *that maintains a constant total current through the laser (uncertainty $\leq 0.03\%$)*.

In order to confirm the effects presented below, each experiment is run for 15 minutes with more than 2500 data points per trial. The positions of the thermocouples are

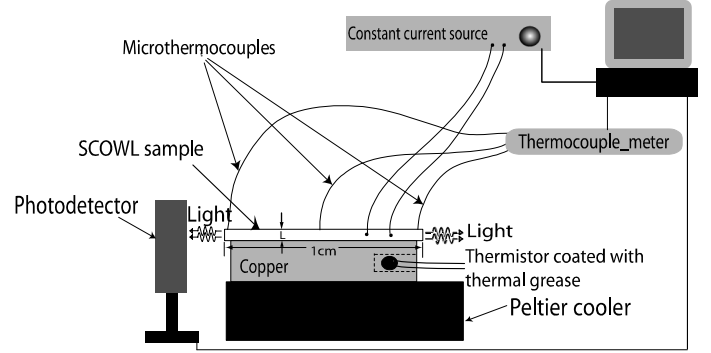


Fig. 1. Schematic of the experimental setup. The feedback-controlled Peltier cooler is connected to a temperature controller, which maintains the copper block heat sink temperature via a thermistor.

exchanged between trials, and the laser orientation on the heat sink is rotated to make sure that the measured fluctuations are not due to the thermocouples themselves or effects within the heat sink.

RESULTS

The difference between the laser's top surface temperature T_{top} and the heat sink temperature T_{sink} at time t is assumed to contain a large-signal term $\Delta T_0(J_0)$ representing a constant temperature difference (time-averaged and spatial-averaged along the laser length x) and a small-signal term dT' representing a time-varying and spatial-varying temperature fluctuation:

$$T_{top}(J_0 + J'(x,t)) - T_{sink} = \Delta T_0(J_0) + dT'(J'(x,t)) \quad (1)$$

where J_0 is the time-averaged and spatial-averaged current density (total injected current divided by the ridge surface area) and $J'(x,t)$ is the current density fluctuation. Note that we consider the laser to be in thermal equilibrium at all times; due to the small size of the laser, we do not consider here time-varying effects such as thermal waves. These effects could be important, however, for large spikes in temperature, and will be investigated in future work.

Finite element models confirm that the thin and flat geometry of the laser justifies a 1D model for heat flow:

$$\Delta T_0(J_0) + dT'(J'(x,t)) = \frac{L}{k} \left[(J_0 + J'(x,t)) \times V - \frac{P_{opt}(J_0)}{A} \right] \quad (2)$$

where V and A are the supply voltage and top contact surface area of the laser. L and k are parameters representing the lumped thermal conductivities of the layers over the total distance L between the laser active region and the heat sink. Note that we neglect here the contribution of the current

density fluctuation J' to the optical power. The convection heat transfer and radiation heat transfer are also neglected due to the small size of the laser and the small magnitude of the measured temperature variations⁹. Finally, we model the fluctuation heat source as only due to nonradiative recombination $J'V$ (where V stays constant), neglecting Joule heating effects.

The two terms on the left hand side of Eq. (2) can be written separately as

$$\Delta T_0(J_0) = \frac{L}{k} \left(J_0 V - \frac{P_{\text{out}}}{A} \right) \quad (3)$$

and

$$dT'(J'(x,t)) = \frac{L}{k} [J'(x,t) \times V] \quad (4)$$

From Eq. (3), the value of L/k can be obtained by solving

$$\frac{L}{k} = \frac{\Delta T_0}{J_0 V - \frac{P_{\text{out}}}{A}} \quad (5)$$

The optical output power P_{out} and spatial-averaged value of L/k are plotted for a range of J_0 in Fig. 2 and Fig. 3. It can be seen that the value of L/k is almost constant, as it should be for heat transfer by conduction alone. The slight decrease in L/k at high bias is likely due to increasing heat transfer by convection⁹.

By combining Eq. (4) and Eq. (5), the variation of current density can be written as

$$J'(x,t) = \frac{dT'(x,t)}{\Delta T_0} \left(J_0 - \frac{P_{\text{out}}}{AV} \right) \quad (6)$$

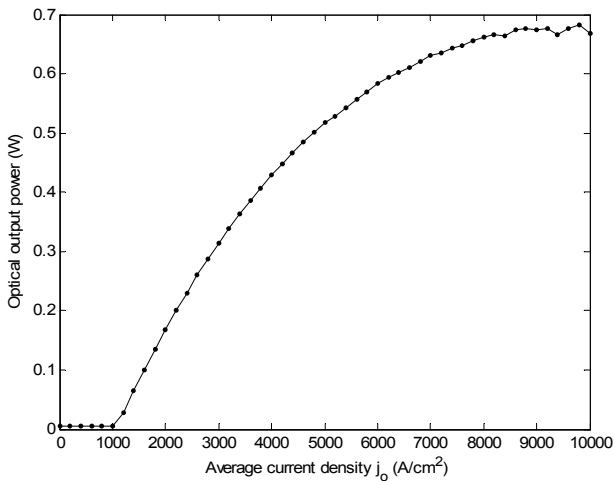


Fig. 2 Optical output power as a function of device current density.

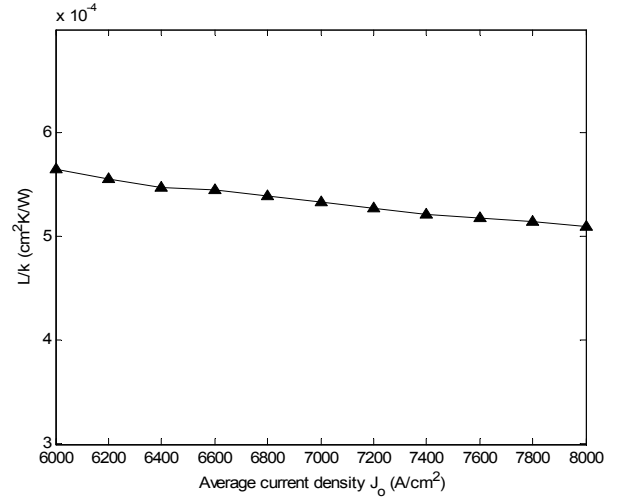


Fig. 3 Measured values of L/k stay constant over the range of bias.

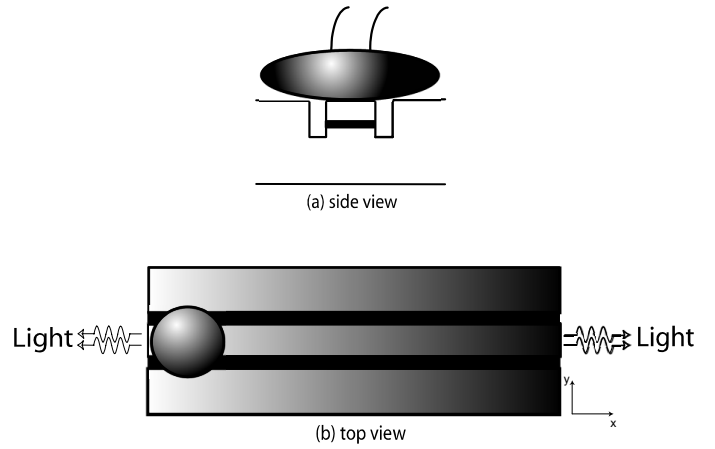


Fig. 4. (a) Side view of the thermocouple on the laser ridge. (b) Top view of the thermocouple on the laser ridge. It can be seen that the size of the thermocouple is a bit larger than the width of the device, but this does not affect the formulation of Eq. (6).

For a given large-signal bias point (J_0, V) , therefore, the time-averaged and spatial-averaged temperature difference across the laser ΔT_0 can be measured. Measuring temperature fluctuations dT' around this bias point, both at different locations on the laser and at different times, *allows one to directly arrive at a spatial profile of the current density injected into the laser surface, as well as its variation in time, through Eq. (6).*

It should be noted that the temperature measured by the thermocouple is the value averaged over the area ($\sim 20\mu\text{m} \times 20\mu\text{m}$) of the thermocouple tip, as shown in Fig. 4. To properly take this effect into account, the exact size and shape of the thermocouple tip must be known, as well as its placement on the laser ridge. Since this is very difficult to ascertain, we make the approximation that the laser surface temperature is proportional to the value measured by the thermocouple.

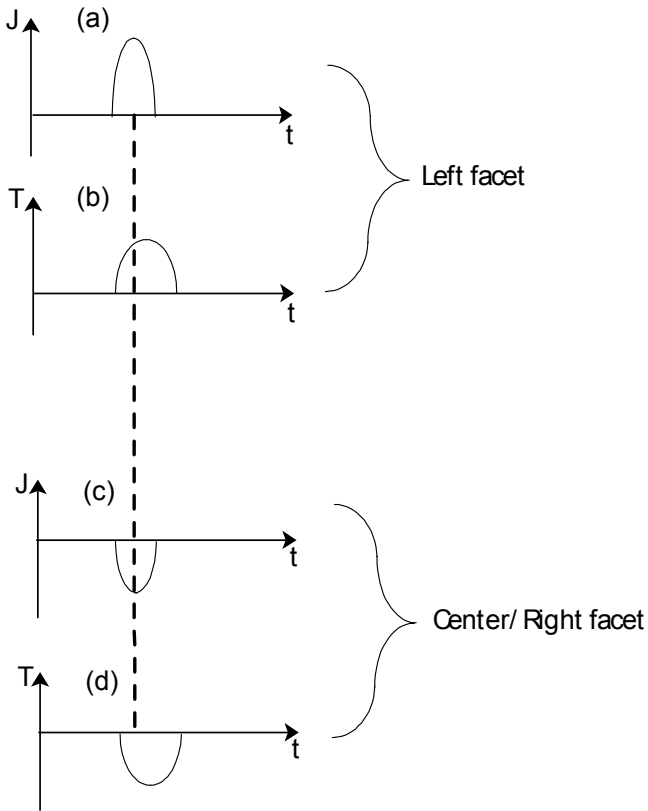


Fig. 5 Illustration of the variation of current density and temperature with time at different locations on the laser. Negative correlation (the temperature in one region mirroring that in another) is due to the current being concentrated at the facet and pulled from the rest of the contact surface.

In this case, Eq. (1) can be rewritten as

$$T_{\text{top}}(J_0 + J'(x, t)) - T_{\text{sink}} = \gamma[\Delta T_0(J_0) + dT'(J'(x, t))] \quad (7)$$

and Eq. (3) and Eq. (4) are similarly

$$\gamma \Delta T_0(J_0) = \frac{L}{k} \left(J_0 V - \frac{P_{\text{out}}}{A} \right) \quad (8)$$

and

$$\gamma dT'(J'(x, t)) = \frac{L}{k} [J'(x, t) \times V] \quad (9)$$

where γ is a proportionality constant. By combining Eq. (8) and Eq. (9), we arrive at Eq. (6) as before. Therefore, although the

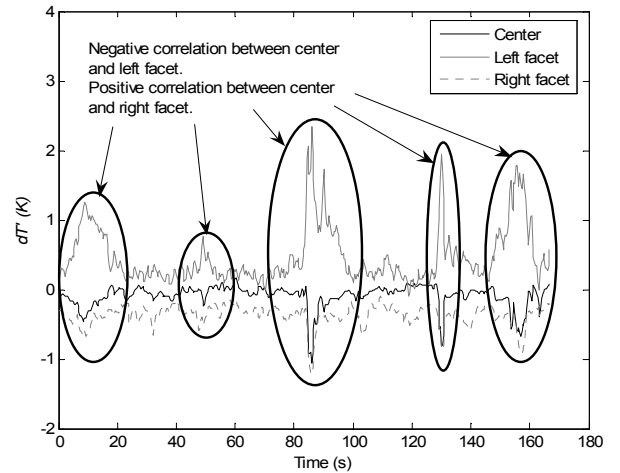


Fig.6 Measured temperature variation with time at $J_0=7000\text{A}/\text{cm}^2$. It shows positive and negative correlations in time (relative to the center) are happening at different locations on the laser surface.

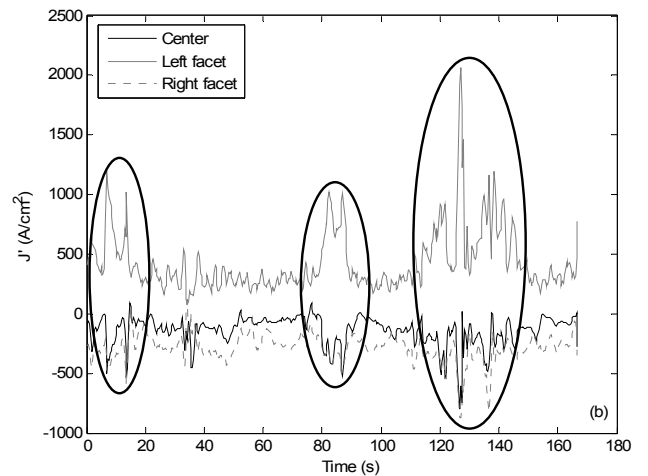
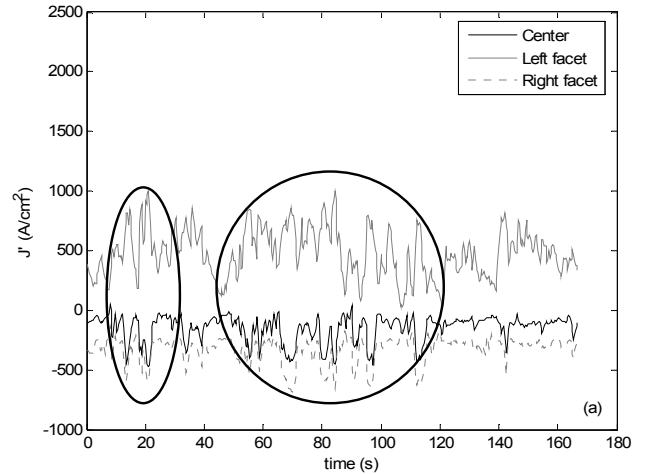


Fig. 7 The magnitude of current density fluctuations increases with increasing J_0 . (a) $J_0 = 6000\text{A}/\text{cm}^2$, (b) $J_0 = 8000\text{A}/\text{cm}^2$.

thermocouples may not be able to measure the exact surface temperature on the laser ridge due to their own size, they still can be used to get an accurate current density map along the laser surface. A further caveat, however, is that the spatial resolution of the current density profile is ultimately determined by the spatial resolution of the thermocouple. Sharp spikes in the current density (and hence temperature) along the length of the laser that are much smaller than the width of the thermocouple will be averaged over the thermocouple area. Therefore, while the measured temperature may rise by several degrees near a laser facet, during a fluctuation, indicating a jump in current density of ~ 2000 A/cm², this is the *average current density increase in the region under the thermocouple*. The current density spike in the submicron region nearest to the facet is likely to be several times as large as the measured value, and the current density increase in the rest of the area under the thermocouple is likely to be smaller than the measured value. This is not a fundamental limitation in the measurement technique, however, only in the size of the thermocouples used.

Fig.5 illustrates how the current density and temperature can change with time at different locations on the laser. As the left facet current density goes up, the surface temperature there will increase; at the same time, the center or right facet current density will go down (since the total current density is held constant by the current source), and as a result the temperature will decrease at the surface there.

Fig. 6 shows the top surface temperature variation dT' at $J_0 = 7000$ A/cm². The left facet dT' fluctuates up to 2.5 K, meaning that the current density changes by up to 1500 A/cm². This represents a fluctuation of 21% of the total injected current density at the left facet, over an area the size of the thermocouple ($\sim 20\mu\text{m}$). If the actual current density spike is concentrated in an area near the facet much smaller than $20\mu\text{m}$ (as is likely), this narrow spike may be much larger than 1500 A/cm². In Fig. 6, it can be seen that the current density increase near the left facet is balanced by the simultaneous current decrease at the center and right facet.

The negative correlation between the left facet and laser center and the positive correlation between the right facet and laser center at $J_0 = 6000$ A/cm² and 8000 A/cm² are shown in Fig. 7. This measurement indicates that current concentration (and possible facet damage) is happening at the left facet but not at the right facet. It can be observed that the magnitude of spikes increases with the J_0 bias point, which is reasonable due to the fact that greater optical power leads to greater facet heating and hence more nonradiative recombination and current concentration. However, the increase in electrical resistance due to increase in temperature may act as the restoring force which causes the current drop back to its original level.

CONCLUSION

In this work, we have demonstrated a new technique to profile the current density along a laser's surface as it evolves in time. While applied here to lasers, this method could prove

useful in electronic devices in general. We have used this technique to examine the current concentration phenomenon that occurs at laser facets during nonradiative recombination heating and that is a main factor in their eventual destruction. From these measurements, we see that in the pre-COD regime, the laser facets experience occasional sharp increases in current density. These spikes, however, fall back down to steady-state values after a time period of ~ 0.5 -3 seconds. The feedback mechanism responsible for reversing this sudden spike in current density before it can lead to COD is likely the increase in electrical resistance at the facet region due to the increase in temperature. If the negative correlation effect and the feedback mechanism that limits it during normal laser operation can be well understood, it may lead to improved laser designs that have improved lifetime through reduced facet current concentration.¹¹

REFERENCES

- [1] Tang, W. C., Rosen H. J., Vettiger, P. and Webb, D. J., 1991, "Raman microprobe study of the time development of AlGaAs single quantum well laser facet temperature on route to catastrophic breakdown," *Applied Physics Letters*, 58 (6), 557-559.
- [2] Chen, G. and Tien, C.L., 1993, "Facet heating of quantum well lasers," *Journal of Applied Physics*, 74 (4), 2167-2174.
- [3] Henry, C. H., Petroff, P.M., Logan, R. A. and Merritt, F.R., 1979, "Catastrophic damage of Al_xGa_{1-x} double-heterostructure laser material," *Journal of Applied Physics*, 50 (5), 3721-3732.
- [4] Menzel, U., Puchert, R., Barwolff, A. and Lau, A., 1998, "Facet heating and axial temperature profiles in high-power GaAlAs/ GaAs laser diodes," *Microelectronic Reliability*, 38, 821-825.
- [5] Spagnolo, V., Troccoli, M., Scamarcio, G., Becker, C., Glastre, G. and Sirtori, C., 2001, "Facet temperature mapping of GaAs/ AlGaAs quantum cascade lasers by photoluminescence microprobe," *Optical Materials*, 17, 219-222.
- [6] Spagnolo, V., Troccoli, M., Scamarcio, G., Scamarcio, Gmachi, C., Capasso, F., Tredicucci, A., Sergent, A.M., Hutchinson, A. L., Sivco, D.L. and Cho, A.Y., 2001, "Temperature profile of GaInAs/ AlInAs/ InP quantum cascade-laser facets measured by microprobe photoluminescence," *Applied Physics Letters*, 78 (15), 2095-2097.
- [7] Tang, C. W., Rosen, H. J., Vettiger, P., and Webb, D. J., 1991, "Evidence for current-density-induced heating of AlGaAs single-quantum-well laser facets," *Applied Physics Letters*, 59 (9), 1005-1007.
- [8] Lürßen, D., Hudgings, J.A., Mayer, P. M. and Ram, R. J., 2005, "Nanoscale thermoreflectance with 10mK temperature resolution using stochastic resonance," 21st Semi-therm Symposium.

- [9] Pipe, K. P. and Ram, R. J., 2003, "Comprehensive heat exchange model for a semiconductor laser diode," IEEE Photonics Technology Letter, 15 (4), 504-506.
- [10] Plant, J.J., Juodawlkis, P. W., Huang, R. K., Donnelly, J. P., Missaggia, L., J. and Ray, K. G., 2005, "1.5- μm InGaAsP-InP slab-coupled optical waveguide lasers," IEEE Photonics Technology Letters, 17 (4), 735-737.
- [11] Horie, H.; Yamamoto, Y.; Arai, N. and Ohta, H, 2000, "Thermal rollover characteristics up to 150 °C of buried-stripe type 980-nm laser diodes with a current injection window delineated by a SiN_x layer," IEEE Photonics Technology Letters, 12 (1), 13-15.